Food Bioprocess Technol (2013) 6:2931–2937
DOI 10.1007/s11947-012-0825-6

COMMUNICATION

Application of Visible and Near Infrared Hyperspectral Imaging to Differentiate Between Fresh and Frozen–Thawed Fish Fillets

Fengle Zhu · Derong Zhang · Yong He · Fei Liu · Da-Wen Sun

Received: 13 October 2011 / Accepted: 7 March 2012 / Published online: 21 March 2012

Abstract The potential of visible and near infrared (VIS/NIR) hyperspectral imaging was investigated as a rapid and nondestructive technique to determine whether fish has been frozen–thawed. A total of 108 halibut (*Psetta maxima*) fillets were studied, including 48 fresh and 60 frozen–thawed (F-T) samples. Regarding the F-T samples, two speeds of freezing (fast and slow) were tested. The hyperspectral images of fillets were captured using a pushbroom hyperspectral imaging system in the spectral region of 380 to 1,030 nm. All images were calibrated for reflectance, followed by the minimum noise fraction rotation to reduce the noise. A region-of-interest (ROI) at the image center was selected, and the average spectral data were generated from the ROI image. Dimension reduction was carried out on the ROI image by principal component analysis. The first three principal components (PCs) explained over 98 % of variances of all spectral bands. Gray-level co-occurrence matrix analysis was implemented on the three PC images to extract 36 textural feature variables in total. Least squares-support vector machine classification models were developed to differentiate between fresh and F-T fish based on (1) spectral variables; (2) textural variables; (3) combined spectral and textural variables, respectively. Satisfactory average correct classification rate of 97.22 % for the prediction samples based on (3) was achieved, which was superior to the results based on (1) or (2). The results turned worse when different freezing rates were taken into consideration to classify three groups of fish. The overall results indicate that VIS/NIR hyperspectral imaging technique is promising for the reliable differentiation between fresh and F-T fish.

Keywords Fresh fish · Frozen–thawed fish · Differentiation · Hyperspectral imaging · Least squares-support vector machine

F. Zhu · Y. He (✉) · F. Liu
College of Biosystems Engineering and Food Science,
Zhejiang University,
866 Yuhangtang Road,
Hangzhou, Zhejiang 310058, People's Republic of China
e-mail: yhe@zju.edu.cn

D. Zhang
Ningbo Institute of Technology, Zhejiang University,
Ningbo 315000, China

D.-W. Sun
Food Refrigeration and Computerised Food Technology,
National University of Ireland,
Belfield, Dublin 4, Ireland

Introduction

Given the perishable nature of fish, extension of its shelf life is necessary and freezing is an excellent and commonly used way. During freezing, storage, and thawing, fish muscles go through a progressive deterioration in nutritive value, texture, and other functional properties (Karoui et al. 2006). When optimum freezing and thawing procedures are adopted, it is not easy to distinguish fresh from frozen–thawed (F-T) fish using sensory evaluation because of the similarity of their physicochemical properties (Duflos et al. 2002). F-T usually has a lower market price than fresh fish due to its inferior quality. Thereby the substitution of F-T for fresh fish is a potential fraudulent practice, and the differentiation of fresh from F-T fish is a significant issue to prevent unfair competition by false labeling.

Numerous methods have been investigated to differentiate between fresh and F-T fish. Although enzymatic and physiological (Duflos et al. 2002), chemical, microbiological, and sensory (Baixas-Nogueras et al. 2007) methods are valid and useful, they are destructive, time-consuming, expensive, and

requiring trained personnel. Among physical methods, the texture analyzers, color instruments, and dielectric testers only describe the change in a single parameter, which is not sufficient to represent for fish freshness change during the whole storage (Nilsen et al. 2002). Satisfactory results were achieved using fluorescence spectroscopy (Karoui et al. 2006), but the sample sizes were not large enough to stand for sample variations.

In recent decades, visible and near infrared (VIS/NIR) spectroscopy has gained great importance in fish quality evaluation due to the advantages of rapid and nondestructive analysis, minimal sample preparation, simultaneous determination of several parameters, and the potential for online usage. It is based on the broad and repetitive absorption of C–H, O–H, and N–H bonds between 400 and 2,500 nm (Li et al. 2008). It was applied to determine chemical composition in fish (Xiccato et al. 2004; Folkestad et al. 2008), differentiate fish quality cultured under different conditions (Costa et al. 2011), and predict fish freshness as storage time on ice (Nilsen et al. 2002). Several studies classified fresh and F-T fish using spectroscopic method. Dry extract spectroscopy by infrared reflection of fresh and F-T fish was performed on the extracted meat juices and differentiated (Uddin and Okazaki 2004). Though correct classification rate (CCR) of 100 % was achieved, extractions were needed and wastes were produced. The best CCR was 87.5 % in the investigation using mid-infrared spectroscopy (Karoui et al. 2007), but the small number of 24 fish samples in total was insufficient to represent for various sample variations in practical applications. Satisfying CCR was obtained using VIS/NIR spectroscopy (Uddin et al. 2005); fish were measured at a location just behind the dorsal fin, but the fixed spatial area was not large enough to stand for information from other part of the fish.

Hyperspectral imaging is a rapid, nondestructive, and non-contact technique which integrates spectroscopy and digital imaging to simultaneously obtain spectral and spatial information. With hyperspectral imaging, a spectrum for each pixel can be obtained and a gray scale image for each narrow band can be acquired, enabling this system to reflect componential and constructional characteristics of an object and their spatial distributions. With respect to fish quality analysis, hyperspectral imaging has been successfully applied in determination of fat and water distribution in fillets (ElMasry and Wold 2008), ridge detection of fillets (Sivertsen et al. 2009), and fish freshness assessment (Chau et al. 2009; Menesatti et al. 2010; Sivertsen et al. 2011). The study on differentiation of fresh and F-T fillets with VIS/NIR hyperspectral imaging analyzed the spectral variables on each grid element on fillets and displayed the CCR as a function of standard spatial position on fillets, without considering the textural information (Sivertsen et al. 2011).

The basic component of hyperspectral images is pixel, which contains two features of brightness value and locations in coordinates. Texture is another significant image feature, corresponding to both brightness value and pixel locations. Image texture reflects changes of intensity values of pixels, and generally a great change in intensity values may denote a change in geometric structure of samples, thus image texture may contain information of geometric structure of samples (Zheng et al. 2006). In fish hyperspectral images, texture reflects cellular structure of fish to some extent and hence can be used as an indicator of fish quality (Gao and Tan 1996).

This work investigated the feasibility of VIS/NIR hyperspectral imaging combined with least squares-support vector machine (LS-SVM) classifiers to differentiate fresh from F-T fish (D1). To investigate the effect of different freezing speeds and temperature on fish quality changes, LS-SVM was also applied to distinguish among fresh, fast frozen–thawed (FF-T), and slow frozen–thawed (SF-T) fish (D2). This study was focus on (a) detecting the spectral differences among fresh, FF-T, and SF-T fish and (b) comparing the performances of LS-SVM models between D1 and D2 based on (1) spectral variables, (2) textural variables, (3) combined spectral and textural variables, respectively.

Materials and Methods

Fish Samples

Fifty-four live halibut (*Psetta maxima*) were purchased from a local market (Hangzhou, China), and transported with sea water to the laboratory. The fish weight ranged between 372 and 580 g (average 512 g) and full length varied from 27.5 to 32 cm (average 30.5 cm). They were immediately slaughtered, bled, de-headed, gutted, cleaned, and iced. Subsequently the fish were filleted and two fillets from the right and left side respectively on the dorsal site were used, resulting in 108 samples altogether. The fillets were trimmed manually for bones, parasites, blood stains, and randomly divided into three groups for further evaluation. The first group of 48 fillets was used as fresh or unfrozen samples soon after slaughtering. The second and third groups of 30 fillets each were stored at the constant temperature of −70 and −20 °C for fast and slow freezing, respectively. During frozen storage, the samples were put in plastic bags to prevent drying of the surface. After 9 days, fillets were thawed overnight at 4 °C as FF-T and SF-T samples, respectively. All samples were allowed to equilibrate to room temperature (20 °C) before scanning by VIS/NIR hyperspectral imaging system. Seventy-two samples of 32 fresh and 40 F-T (20 FF-T and 20 SF-T) were randomly selected to create the calibration set; the remaining 36 samples of 16 fresh and 20 F-T (10 FF-T and 10 SF-T) formed the prediction set.

Hyperspectral Imaging System and Image Acquisition

The VIS/NIR hyperspectral imaging system was employed to capture hyperspectral images of fillets in reflectance mode. The system consists of a spectrograph (ImSpector V10E, Specim, Finland), a 12-bit CCD camera (Hamamatsu, Japan), two 150 W tungsten halogen lamps (Fiber-Lite DC950 Illuminator, Dolan Jenner Industries Inc, USA) for illumination, a conveyer belt (Isuzu Optics Corp, Taiwan, China) driven by a stepping motor, and a computer with data acquisition and preprocessing software (Spectral Image-V10E, Isuzu Optics Corp, Taiwan, China). The spectral resolution is 2.8 nm in 380–1,030 nm. The camera, fitting with a C-mount 23-mm lens, has 672×512 (spatial × pectral) pixels. The system scans a single spatial line of the sample, and the reflected light was dispersed by the spectrograph in spatial–spectral (672×512) axis. To obtain a three-dimensional hypercube, the sample has to be moved along another spatial axis. The speed of the conveyer belt was adjusted as 35 mm/s to synchronize with the camera scanning and achieve a square pixel. With this pushbroom configuration, each fillet was individually transported by the conveyor belt to be scanned line by line with 7 ms exposure time, and upon entering the field of view, the acquisition of a hyperspectral image began. Each image consisted of 512 congruent images at 512 contiguous spectral bands. The hyperspectral images were stored in raw format and exported to the Environment for Visualizing Images V4.6 software (ITT Visual Information Solutions, Boulder, USA) for subsequent processing.

Image Calibration and Denoising

All raw hyperspectral images (I_0) were calibrated for reflectance to minimize differences among samples due to sensor response and illumination. The dark reference image (B) of approximately 0 % reflectance was acquired for removing the influence of dark current in the camera by turning off the light source together with covering the camera lens completely with its opaque cap. The image of a white Teflon tile with about 100 % reflectance was used as the white reference image (W). The calibrated hyperspectral image (I) in the unit of relative reflectance (%) was calculated as:

$$I = \frac{I_0 - B}{W - B} \times 100 \quad (1)$$

Due to the insufficient light intensity of halogen lamps at the starting spectral region, obvious noise was observed at the first 62 bands of calibrated images. Thus, these bands were eliminated, and spectral region from band 63 to 512, corresponding to the wavelength range of 456–1,030 nm, was employed. Minimum noise fraction (MNF) rotation was implemented on the 450 bands of calibrated images to reduce spectral noise and maximize signal-to-noise ratio. MNF is a linear transformation, consisting of two cascaded principal component analysis (PCA) rotations. Noise was effectively removed from the hyperspectral image data by forward transforming to the MNF space, rejecting the noise-dominated components, then inverse MNF transforming into the original data space (Green et al. 1988). All denoised images were used as the basis for further analysis.

Spectral and Textural Variables Extraction

A region-of-interest (ROI) of size 300×100 pixels around the center of the image was selected. All spectral reflectance curves of all pixels identified by the ROI image were averaged to generate only one mean spectrum standing for the sample. The same procedure was repeated for all ROI images, and a spectral matrix 108 samples × 450 bands was constructed.

To reduce spectral dimension, PCA was carried out for all ROI images. PCA applies a linear transformation to decompose the spectral data into several principal components (PCs), which are uncorrelated and account for the most common spectral variations. The first three PC images were saved and exported to the MATLAB V7.8 software (The Math Works, Natick, USA) (Li et al. 2008).

Gray-level co-occurrence matrix (GLCM) is a texture analysis technique which is based on the usage of second-order statistics of co-occurrence matrix. In this study, GLCM were executed on the PC images to extract textural variables. GLCM was created by calculating how often a pixel with a particular gray level value occurs at a specified distance and angle from its adjacent pixels. The parameters in creating the GLCM were the default values in MATLAB. The distance equals to 1 because many pixels would be out of counting in the process of generating GLCM in case of large distance. As the image texture was less affected by different angles, the angle was 0° to simplify computation. The gray level was 8 to reduce calculation time and avoid too many zeros in the GLCM. For each PC image, 12 second-order statistical textural variables were computed based on GLCM, which were: contrast, correlation, angular second moment, homogeneity, variance, entropy, sum average, sum variance, sum entropy, difference average, difference variance, and difference entropy (Haralick et al. 1973). In total, 36 textural variables were derived from three PC images for each ROI image. The calculation of textural variables for all PC images of all samples produced a textural matrix of 108 samples × 36 variables.

Least Squares-Support Vector Machine

Support vector machine (SVM) is a powerful methodology for solving problems in nonlinear classification, function estimation, and pattern recognition. SVM uses kernel function to map the data input space to a high-dimensional feature

space where an optimal hyperplane can be constructed to perform separation. LS-SVM (Suykens et al. 2002) is a reformulation of standard SVM, which works with least squares linear cost function. It not only owns the advantage of good generalization performance as SVM but also possesses simpler structure and shorter optimization time. When using LS-SVM, three crucial problems needed to be resolved, namely the selection of optimal input subset, appropriate kernel function, and optimum kernel parameters. The inputs of LS-SVM classifiers were the extracted (1), (2), and (3), respectively. The kernel function was the radial basis function (RBF) kernel because it is a compactly supported kernel and capable of reducing the computational complexity of training procedure while giving good performance under general smoothness assumptions. The two-step grid search and leave-one-out cross-validation was employed for the optimization of regularization parameter gam (γ) and RBF kernel bandwidth parameter sig^2 (σ^2).

Results and Discussion

Overview of the Spectra

The mean VIS/NIR absorbance (log 1/R) curves for fresh, FF-T, and SF-T fish are displayed in Fig. 1a. The general trends of the spectral curves for three categories of fish were similar. However, the overall absorbance level was found to decrease in F-T samples, which was in accordance with the results in other investigations (Uddin and Okazaki 2004; Uddin et al. 2005). The spectral differences between fresh and F-T samples involved the baseline shift, which might have been induced by light scattering due to variation in fillets thickness. Besides the effects of baseline shift, the differences between spectra were related to fish quality changes, which mainly referring to the alterations in physical structure of at least the surface layer of fish as well as the biochemical and textural changes in fish in freezing, frozen storage, and thawing, which will be discussed in detail in the following passage. The storage time also had some influences on fish quality changes. However, under the condition of low temperatures (−70 or −20 °C), fish quality changed slowly with the passage of frozen storage time because of the low activity of catabolic enzymes and microorganisms. Therefore, compared with storage time, freezing preservation and thawing had more effects on fish quality changes.

More specifically, during freezing, storage, and thawing of fish, ice crystals growth caused tissue damage and texture deterioration, as well as the disruption and leakage of various cellular organelles (Benjakul et al. 2003). Formaldehyde, resulting from decomposition of trimethylamine oxide, reacted with fish proteins, not only resulting in the acceleration of protein denaturation, but also leading to the toughening and texture deterioration of fish muscle (Baixas-Nogueras et al. 2007). Successive protein denaturation gave rise to the lower water holding capacity of protein (Benjakul et al. 2003). For the above reasons, water was more easily released from F-T fish muscle. The less absorbance of F-T samples was partly attributed to the reduced water contents. Also, smaller fractions in F-T fish, arising from degradation of protein, lipid, glycogen, and trimethylamine oxide, gave increased light scattering in general, causing lower absorbance of F-T than fresh fish. The lipid oxidation and loss of vitamins were other important factors leading to quality deterioration of F-T fish. Moreover, some inconspicuous changes in the color of F-T fish existed because, in frozen storage, more heme pigments were oxidated into oxidized heme pigments which had darker color. Meanwhile, as mentioned above, fish texture also underwent some changes in this process. The existence of these differences suggested that it might be possible to detect F-T treatment by spectroscopic and textural analysis for hyperspectral images.

The quality of F-T fish was closely correlated with freezing and thawing processes. The rate of freezing and formation of

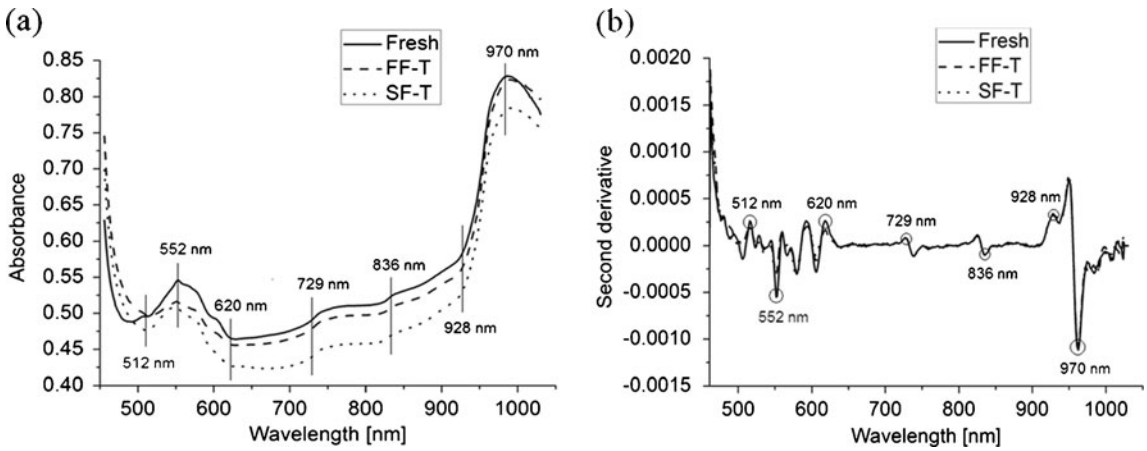

Fig. 1 The mean VIS/NIR absorbance curves (**a**) and second derivative spectra (**b**) for fresh, FF-T, and SF-T fish. Ranges of standard deviation (±) for each mean spectral curve: 0.02102~0.05063 for fresh, 0.02083~0.04449 for FF-T, and 0.02231~0.05093 for SF-T fish

small ice crystals during freezing was critical to minimize tissue damage and drip loss in thawing (Li and Sun 2002). Compared with slow freezing, more ice crystals formed in fast freezing; they were smaller and distributed more evenly, resulting in less tissue damage due to their smaller expansive force. In the subsequent thawing process of fast frozen fish, the thawed water permeated into fish tissue more easily, which was more beneficial to the preserving of fish quality and nutritional value. Consequently, compared with SF-T, the quality and spectral characteristics of FF-T were more similar with fresh fish, and the total absorbance level of FF-T was higher than SF-T fish.

Distinct separation of fresh, FF-T, and SF-T fish occurred at several absorption bands throughout the spectra. To present the characteristic peaks and troughs more clearly, the Savitzky–Golay second order derivative of absorbance data for fresh, FF-T, and SF-T fish is shown in Fig. 1b, with smoothing points of 11. Besides the function of reducing the effects of baseline offsets, the second derivative spectra sharpened spectral features so that broad and overlapping absorption bands could be better distinguished. Peaks in original spectra usually changed sign and turned to negative troughs in second derivative spectra. Water absorbed strongly in some specific wavelengths, which usually exhibited a broad band because of H bonding interactions with itself and with other components in fish. According to Fig. 1b, the prominent band at around 970 nm for water arose from the second overtone band of O–H stretch and bending mode. The weaker absorptions near 729 nm, originating from the O–H stretch third overtone band in water, could be assigned. The weaker absorptions at about 836 nm related to O–H bond in water could also be distinguished. In addition, a minor peak located at 928 nm was present, which corresponded to the third overtone C–H stretch in lipid and protein (Osborne and Fearn 1986). Furthermore, the wavelength around 552 nm corresponding to the absorption of heme pigments such as hemoglobin and myoglobin was negatively correlated with the bands at approximately 512 and 620 nm which were due to the absorptions by oxidized heme pigments such as methemoglobin and metmyoglobin (Sivertsen et al. 2011). This was because the amount of heme pigments was negatively associated with oxidized heme pigments in both fresh and F-T fish. The spectral changes at 970, 729, 836, 928, 552, 512, and 620 nm among fresh, FF-T, and SF-T fish made the differentiation more well-founded.

Differentiation Between Fresh and F-T Fish

The main steps in the whole procedure of hyperspectral image analysis are illustrated in Fig. 2. The first three PC images were selected for each ROI image in respect that they had Eigen values significantly greater than zero (Johnson 1998) and accounted for over 98 % of the cumulative spectral variances. Thus, the 36 textural variables extracted from the three PC images could stand for the textural information in ROI image.

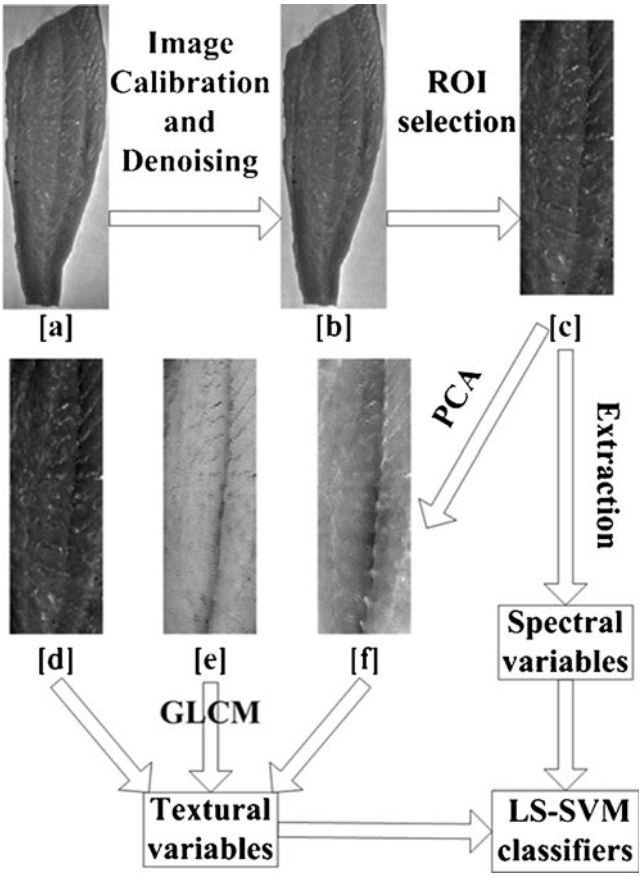

Fig. 2 Flowchart of main steps in the whole procedure of hyperspectral image analysis. [*a*] Raw image, [*b*] calibrated and denoised image, [*c*] ROI image, [*d–f*] PC images 1 through 3

The performances of LS-SVM classifiers were evaluated by CCR. Table 1 presents the CCR for prediction set in D1 and D2 based on (1), (2), and (3), respectively. The (1) represented the componential and structural characteristics of molecules in fish; (2) reflected the spatial information and cellular structure of fish; and (3) made full advantages of hyperspectral imaging in integrating spectroscopy and digital imaging in one system. The average CCR and the CCR for

Table 1 CCR (in percent) for prediction set in D1 and D2 based on (1) spectral variables, (2) textural variables, and (3) combined spectral and textural variables, respectively

Category	D1			D2			
	Fresh	F-T	Average	Fresh	FF-T	SF-T	Average
(1)	93.75	90	91.67	93.75	70	70	80.56
(2)	87.5	95	91.67	81.25	50	50	63.89
(3)	93.75	100	97.22	93.75	70	70	80.56

each category of all three models in D1 were satisfactory. The average CCR of both 91.67 % was observed for models based on (1) and (2). Improved performance was obtained for model based on (3) with average CCR of 97.22 % that was better than the CCR of 87.8 % for all regions on cod fillets using VIS/NIR hyperspectral imaging (Sivertsen et al. 2011). It was obvious that both spectral and textural information contributed significantly to D1, indicating that both physicochemical and textural characteristics in fish changed greatly in freezing, storage, and thawing.

The results for all three models in D2 were worse than those for the corresponding models in D1. Using only (1), in D2, the average CCR reduced to 80.56 %, the CCR for fresh maintained the same (93.75 %) as that in D1, and both of the CCR for FF-T and SF-T was not high (70 %). This implied that fresh samples were well separated from others based on (1), but the spectra of FF-T and SF-T were similar to some degree. Using only (2), compared with D1, the average CCR in D2 dropped from 91.67 to 63.89 %, the CCR for fresh reduced from 87.5 to 81.25 %, and both of the CCR for FF-T and SF-T only reached 50 %. This indicated that fresh samples were distinguished from others based on (2), whereas the textures of FF-T and SF-T were too similar to be classified. In D2, the acceptable CCR for models based on (3) and (1) was similar although (2) was added to (3) in comparison with (1), indicating the major contribution of (1) and minor contribution of (2) to D2. Furthermore, different freezing speeds and temperature had little effects on the changes of fish texture while causing great changes in physicochemical characteristics in fish.

Earlier spectroscopic researches on fish (Uddin and Okazaki 2004; Uddin et al. 2005; Karoui et al. 2007) only made advantages of spectral information since no spatial and textural information was included in the data. Previous studies on fish using hyperspectral imaging exploited spectral and spatial information without fully capitalizing on the spatial arrangement of brightness values of pixels (ElMasry and Wold 2008; Chau et al. 2009; Menesatti et al. 2010; Sivertsen et al. 2011). Thereby, the utilization and combination of both spectral and textural information of hyperspectral images was a more meaningful exploration. However, as a preliminary and mechanism study, the spectra extraction was based on ROI identification. More work should be carried out with some objective and automated approaches. Furthermore, to be more close to practical situation, the quality changes of fresh or F-T fish during storage after slaughtering or thawing will be considered in the following investigations. In addition, further researches should be done to extend to a larger number of samples for validation; study the effect of sample handling, halibut size, season, and fishing ground; investigate more sophisticated pretreatments for spectral data, as well as improve the robustness and rigorousness of LS-SVM models before VIS/NIR hyperspectral imaging can be applied as an online and practical method for detecting F-T fish.

Conclusion

The overall results indicate that VIS/NIR hyperspectral imaging combined with LS-SVM has the potential to be used as an online technique for rapid and nondestructive differentiation of fresh from F-T fish. The overall absorbance level was lower in F-T than fresh fish. High average CCR of 97.22 % was obtained based on (3), which was better than the average CCR of 91.67 % based on (1) or (2). The CCR in D2 was worse than D1 mainly because of the similarity in the textures of FF-T and SF-T fish.

Acknowledgments This study was supported by the 863 National High-Tech Research and Development Plan (Project no: 2011AA100705) and the Fundamental Research Funds for the Central Universities.

References

Baixas-Nogueras, S., Bover-Cid, S., Veciana-Nogués, M. T., & Vidal-Carou, M. C. (2007). Effects of previous frozen storage on chemical, microbiological and sensory changes during chilled storage of Mediterranean hake (*Merluccius merluccius*) after thawing. *European Food Research and Technology, 226*, 287–293.

Benjakul, S., Visessanguan, W., Thongkaew, C., & Tanaka, M. (2003). Comparative study on physicochemical changes of muscle proteins from some tropical fish during frozen storage. *Food Research International, 36*, 787–795.

Chau, A., Whitworth, M., Leadley, C., & Millar, S. (2009). Innovative sensors to rapidly and non-destructively determine fish freshness. Campden BRI. Report No. CMS/REP/110284/1.

Costa, C., D'Andrea, S., Russo, R., Antonucci, F., Pallottino, F., & Menesatti, P. (2011). Application of non-invasive techniques to differentiate sea bass (*Dicentrarchus labrax,* L. 1758) quality cultured under different conditions. *Aquaculture International, 19*, 765–778.

Duflos, G., Le Fur, B., Mulak, V., Becel, P., & Malle, P. (2002). Comparison of methods of differentiating between fresh and frozen–thawed fish or fillets. *Journal of the Science of Food and Agriculture, 82*, 1341–1345.

ElMasry, G., & Wold, J. P. (2008). High-speed assessment of fat and water content distribution in fish fillets using online imaging spectroscopy. *Journal of Agricultural and Food Chemistry, 56*, 7672–7677.

Folkestad, A., Wold, J. P., Rørvik, K. A., Tschudi, J., Haugholt, K. H., Kolstad, K., & Mørkøre, T. (2008). Rapid and non-invasive measurements of fat and pigment concentrations in live and slaughtered Atlantic salmon (*Salmo salar* L.). *Aquaculture, 280*, 129–135.

Gao, X., & Tan, J. (1996). Analysis of expended-food texture by image processing part I: geometric properties. *Journal of Food Processing Engineering, 19*, 425–444.

Green, A. A., Berman, M., Switzer, P., & Craig, M. D. (1988). A transformation for ordering multispectral data in terms of image quality with implications for noise removal. *IEEE Transactions on Geoscience and Remote Sensing, 26*, 65–74.

Haralick, R. M., Shanmugam, K., & Dinstein, I. (1973). Textural features for image classification. *IEEE Transactions on Systems, Man, and Cybernetics, 3*, 610–621.

Johnson, R. A. (1998). *Applied multivariate methods for data analysis*. New York: Duxbury.

Karoui, R., Thomas, E., & Dufour, E. (2006). Utilisation of a rapid technique based on front-face fluorescence spectroscopy for differentiating between fresh and frozen–thawed fish fillets. *Food Research International, 39*, 349–355.

Karoui, R., Lefur, B., Grondin, C., Thomas, E., Demeulemester, C., Baerdemaeker, J. D., & Guillard, A.-S. (2007). Mid-infrared spectroscopy as a new tool for the evaluation of fish freshness. *International Journal of Food Science and Technology, 42*, 57–64.

Li, B., & Sun, D. W. (2002). Novel methods for rapid freezing and thawing of foods—a review. *Journal of Food Engineering, 54*, 175–182.

Li, X. L., He, Y., & Wu, C. Q. (2008). Non-destructive discrimination of paddy seeds of different storage age based on Vis/NIR spectroscopy. *Journal of Stored Products Research, 44*, 264–268.

Menesatti, P., Costa, C., & Aguzzi, J. (2010). Quality evaluation of fish by hyperspectral imaging. In D.-W. Sun (Ed.), *Hyperspectral imaging for food quality analysis and control* (pp. 273–294). London: Academic.

Nilsen, H., Esaiassen, M., Heia, K., & Sigernes, F. (2002). Visible/near-infrared spectroscopy: a new tool for the evaluation of fish freshness? *Journal of Food Science, 67*, 1821–1826.

Osborne, B. G., & Fearn, T. (1986). *Near infrared spectroscopy in food analysis*. New York: Longman Scientific & Technical.

Sivertsen, A. H., Chu, C. K., Wang, L. C., Godtliebsen, F., Heia, K., & Nilsen, H. (2009). Ridge detection with application to automatic fish fillet inspection. *Journal of Food Engineering, 90*, 317–324.

Sivertsen, A. H., Kimiya, T., & Heia, K. (2011). Automatic freshness assessment of cod (*Gadus morhua*) fillets by Vis/Nir spectroscopy. *Journal of Food Engineering, 103*, 317–323.

Suykens, J. A. K., Van Gestel, T., De Brabanter, J., De Moor, B., & Vandewalle, J. (2002). *Least squares support vector machines*. Singapore: World Scientific.

Uddin, M., & Okazaki, E. (2004). Classification of fresh and frozen–thawed fish by near-infrared spectroscopy. *Journal of Food Science, 69*, C665–C668.

Uddin, M., Okazaki, E., Turza, S., Yumiko, Y., Tanaka, M., & Fukuda, Y. (2005). Non-destructive visible/NIR spectroscopy for differentiation of fresh and frozen–thawed fish. *Journal of Food Science, 70*, C506–C510.

Xiccato, G., Trocino, A., Tulli, F., & Tibaldi, E. (2004). Prediction of chemical composition and origin identification of European sea bass (*Dicentrarchus labrax* L.) by near infrared reflectance spectroscopy (NIRS). *Food Chemistry, 86*, 275–281.

Zheng, C. X., Sun, D. W., & Zheng, L. Y. (2006). Recent applications of image texture for evaluation of food qualities—a review. *Trends in Food Science and Technology, 17*, 113–128.